

Adaptive Transmission for Mobile Packet-Radio Networks: Protocol Performance vs. Capacity Limits

Michael B. Pursley and Thomas C. Royster, IV, Clemson University
Jason S. Skinner, The Citadel

Abstract—Protocols for adapting the rate of an error-control code in a packet radio network are described and performance evaluations are given for channels with time-varying parameters that are modeled by finite-state Markov chains. The performance of each protocol is compared with the performance of an ideal protocol that has perfect channel-state information and employs a set of capacity-achieving codes of the same rates as the codes available to our protocol. The statistics used for adaptation by our protocol are derived from the demodulator and decoder in the receiving radio, and they are provided to the transmitting radio by a few bits that are included in each acknowledgment packet.

I. INTRODUCTION

In order to maintain high throughput in wireless packet radio networks with time-varying channels, it is necessary to adapt the rate of the error-control code as the channel changes. We describe protocols for accomplishing this task, and we evaluate their performance for dynamic channels with variations governed by finite-state Markov chains. Our protocol is not given any channel-state information; instead, the adaptation is driven by statistics that are derived in the receiver. We assume the radios employ half-duplex packet transmission, which implies that feedback information from the destination cannot be received during the transmission of a packet. The feedback for our protocols is provided by acknowledgment packets. For comparison, we also determine the performance of an ideal protocol that is given perfect channel-state information. Capacity bounds are obtained by coupling the ideal protocol with a set of capacity-achieving codes that have the same rates as the set of codes employed by our protocol.

The system model is illustrated in Fig. 1. All forms of coding and modulation in this paper are examples of bit-interleaved coded modulation [2]. Performance results are given for adaptive-rate coding with product codes, S-random [3] or helical interleaving, and soft-decision iterative decoding. One terminal, referred to as the *source*, wishes to send one or more packets to another terminal, referred to as the *destination*. In this paper, a *packet* is an information packet unless specified otherwise (e.g., an acknowledgment packet). Each packet contains a payload, which is the message portion of the packet, and a header that includes a field for specifying the error-control code that is used to encode the message and a field that carries a few bits of feedback information used to provide the source with the adaptation statistics. The number of binary code symbols is constant, independent of the code rate, so the number of information bits per packet varies with the code rate.

This research was supported by the Office of Naval Research under Grant N00014-04-1-0563. Thomas Royster received additional support from a National Science Foundation Graduate Research Fellowship.

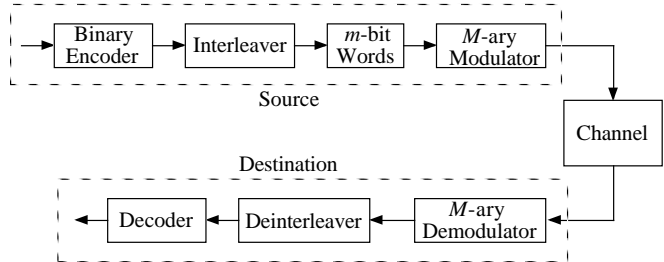


Fig. 1. System Model

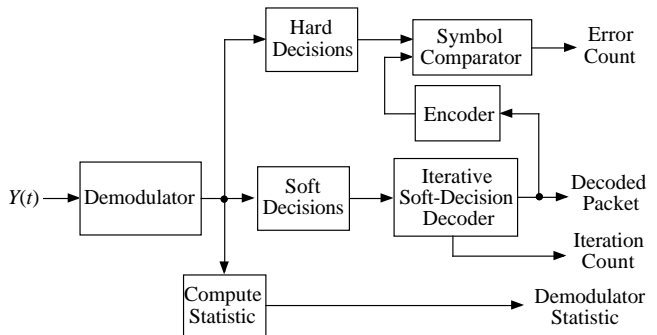


Fig. 2. Extraction of statistics for use in adaptive transmission

The statistics derived in the receiver are illustrated in Fig. 2. The *iteration count for a received word* is the number of iterations performed by the decoder for the word, and the *iteration count for a packet* is the average of the iteration counts for the words in the packet. The *error count* for a packet is the number of errors in the binary symbols that are derived from hard decisions made at the demodulator output. As illustrated in Fig. 2, the error count can be determined for a correctly decoded packet by encoding the information symbols at the output of the soft-decision decoder and comparing the resulting code symbols with the hard-decision demodulated binary symbols. If there are multiple code words per packet, then the error count for the packet is the sum of the error counts for the received words. The type of *demodulator statistic* that is employed for adaptation depends on the modulation format, and it may depend on the soft-decision metric that is used for decoding.

II. CHANNEL MODELS

For a channel with no fading, the energy per information bit is denoted by \mathcal{E}_b and the energy per binary code symbol is denoted by \mathcal{E} . If the error-control code has rate r , then the two energies are related by $\mathcal{E} = r\mathcal{E}_b$. For QAM, these energies are not the same for all points in the constellation,

so \mathcal{E}_b and \mathcal{E} denote the average energies for the information bits and binary code symbols, respectively. The receiver's thermal noise is modeled as full-band white Gaussian noise with one-sided power spectral density N_0 . Although each of our channel models includes full-band additive white Gaussian noise (AWGN), we reserve the phrase *AWGN channel* for a channel that has no fading and no other noise or interference. Power and energy ratios are expressed in decibels (dB) by defining such parameters as $\text{ENR} = 10 \log_{10}(\mathcal{E}_b/N_0)$ and $\text{SENR} = 10 \log_{10}(\mathcal{E}/N_0)$.

For frequency-hop communications over a channel with partial-band interference, the interference is modeled as band-limited white Gaussian noise that occupies a fraction ρ of the available frequency band. The one-sided power spectral density for the band-limited noise is $\rho^{-1}N_I$ in the frequency slots that have interference, and it is zero in the remaining fraction $1-\rho$ of the slots. The total power in the interference is proportional to N_I , but it is independent of ρ . The bit energy to interference density ratio in dB is $\text{EIR} = 10 \log_{10}(\mathcal{E}_b/N_I)$ and the symbol energy to interference density ratio in dB is $\text{SEIR} = 10 \log_{10}(\mathcal{E}/N_I)$.

For the Rician fading channel, the energy per binary code symbol for the specular component is denoted by \mathcal{E}_s , the average energy per binary symbol in the diffuse component is \mathcal{E}_d , and the average total energy per binary symbol for the received signal is \mathcal{E}_a . The *Rician fading parameter* γ is the ratio of the average energy in the diffuse component to the energy in the specular component; that is, $\gamma^2 = \mathcal{E}_d/\mathcal{E}_s$. The AWGN channel ($\gamma^2=0$) and Rayleigh fading channel ($\gamma^2=\infty$) are obtained as special cases.

III. ADAPTATION OF THE CODE RATE

Each protocol uses feedback information from the destination that consists of one or more of the adaptation statistics that are derived in the demodulator and decoder (illustrated in Fig. 2). In our preferred mode of operation, the destination sends an acknowledgment packet in response to each packet that it receives from the source. If an acknowledgment is not received, the source retransmits the packet, perhaps using a code of lower rate. In one alternative mode, which is not evaluated in this paper, a single acknowledgment packet is sent in response to a specified number of consecutive packets from the source.

The *expected throughput* is the number of information bits per packet times the probability of success for the packet. The performance measure for a session in which several packets are sent from the source to the destination is the *throughput* for the session, which is defined as the total number of information bits in packets that are decoded correctly at the destination divided by the total number of packet transmissions that are made by the source (including retransmissions). An information bit is not counted in the numerator of the throughput expression unless the entire packet is decoded correctly. All packet transmissions, whether they are decoded correctly or not, are counted in the denominator, so the protocol is penalized for failed packets.

The protocol strives to achieve the best balance between a high-rate code, which represents a larger number of information

bits per packet but may have a lower success probability, and a low-rate code, which may have a higher success probability but carries fewer information bits in each packet. The best choice depends on the channel state, which is unknown to the protocol. The protocol selects the code for the next packet transmission according to one or more adaptation statistics from the previous packet transmission. In addition to the turbo product code, a high-rate CRC code is employed to verify the decoder output is correct before any adaptation statistics are evaluated. If the previous transmission was not decoded correctly, then the code rate is reduced by one step if possible (i.e., if the code of lowest rate was not used); otherwise, the code rate is unchanged for the next transmission. If the packet is decoded correctly, then the selection of the code rate for the next packet is based on comparisons of the adaptation statistics with the protocol's adaptation parameters. Examples of the adaptation parameters and the comparisons that are made are given in [7]–[9] and [11].

IV. CODE PERFORMANCE AND CAPACITY LIMITS FOR STATIC CHANNELS

The protocol has available a set $\{C_i : 1 \leq i \leq n_c\}$ of error-control codes of rates r_1, r_2, \dots, r_{n_c} in increasing order. We consider fixed-length packets with n_b binary code symbols per packet. If a packet is encoded with code C_i , then it represents $k_i = r_i n_b$ bits of information. Our numerical performance results are for an adaptive coding system that has a set of five turbo product codes and transmits information in packets with $n_b = 4096$ binary code symbols per packet. The block length is 4096 for each of the three *primary codes* C_2 , C_3 , and C_5 , which have 1331, 2028, and 3249 information bits per block, respectively. The corresponding approximate rates are 0.325, 0.495, and 0.793. Code C_1 has block length 2048 with 484 information bits per block, which gives an approximate rate of 0.236. The block length for code C_4 is 1024, and it has 676 information bits per block for an approximate rate of 0.660. There is one code word per packet for each of the primary codes, two code words per packet for C_1 and four code words for packet for C_4 . Encoders and iterative decoders for all five codes are available on a single chip [1], which makes this set of codes very attractive for use in adaptive-rate coding.

For systems that demodulate coherently, the log-likelihood-ratio (LLR) metric (e.g., see [4]–[6]) is used for all modulation formats except QAM. A simpler distance metric [5] with approximately the same performance as the LLR metric is employed for QAM. For noncoherent demodulation of binary orthogonal signals, we employ the log-ratio metric, which is the logarithm of the ratio of the outputs of the two noncoherent detectors (e.g., envelope detectors).

In order to compare the performance of our protocol with the capacity bounds for adaptive-rate coding protocols, we must evaluate the capacity limit for each combination of modulation format and channel model. For most channels, we define the *capacity limit* for rate r to be the minimum value of ENR for which there exist codes of rate r that provide an arbitrarily small error probability as their block lengths increase to infinity (i.e., the Shannon capacity interpreted as a lower bound on

	0.236	0.325	0.495	0.660	0.793
$\Lambda_c(r)$	-0.8	-0.5	0.2	1.0	2.0
$\Gamma_c(r)$	1.5	1.1	1.7	2.9	2.9
$\Delta_c(r)$	2.3	1.6	1.5	1.9	0.9
$\Lambda_n(r)$	7.2	6.9	6.7	6.9	7.4
$\Gamma_n(r)$	8.8	8.3	8.0	8.3	8.2
$\Delta_n(r)$	1.6	1.4	1.3	1.4	0.8
$\Lambda_{16,Q}(r)$	0.6	1.2	2.3	3.7	5.0
$\Gamma_{16,Q}(r)$	3.4	3.1	4.2	5.7	6.2
$\Delta_{16,Q}(r)$	2.8	1.9	1.9	2.0	1.2
$\Lambda_{64,Q}(r)$	1.9	2.8	4.7	6.6	8.5
$\Gamma_{64,Q}(r)$	5.4	5.4	7.0	9.0	9.8
$\Delta_{64,Q}(r)$	3.5	2.6	2.3	2.4	1.3
$\Lambda_{64,B}(r)$	2.2	1.7	1.2	1.2	1.4
$\Gamma_{64,B}(r)$	3.7	2.9	2.2	2.9	2.1
$\Delta_{64,B}(r)$	1.5	1.2	1.0	1.7	0.7

TABLE I

Capacity limits and requirements for 10^{-2} packet error probability on an AWGN channel

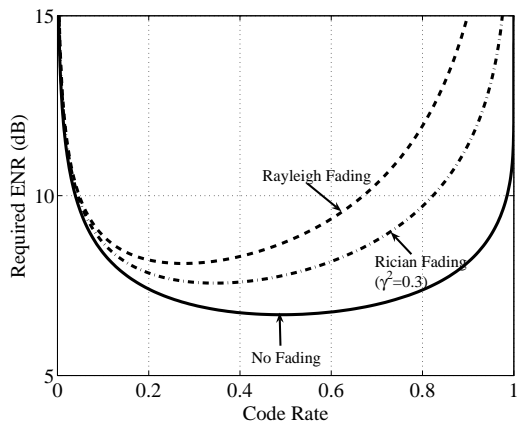


Fig. 3. Capacity limits for binary orthogonal modulation, noncoherent demodulation, and frequency hopping.

ENR). For certain channels, such as those with partial-band interference, we hold one parameter constant (e.g., ENR) and determine the minimum value of another parameter (e.g., EIR) that is required to achieve an arbitrarily small error probability.

We denote the capacity limit in dB by $\Lambda_c(r)$ for coherent demodulation of binary antipodal signals (e.g., optimum receivers for coherent BPSK or coherent QPSK) and by $\Lambda_n(r)$ for noncoherent demodulation of binary equal-energy orthogonal signals (e.g., binary FSK). The capacity limits for coherent demodulation of M -QAM and M -biorthogonal signals are denoted by $\Lambda_{M,Q}(r)$ and $\Lambda_{M,B}(r)$, respectively.

For the turbo product code of rate r , the values of ENR required to provide a packet error probability of 10^{-2} for coherent binary antipodal, noncoherent binary orthogonal, coherent M -QAM, and coherent M -biorthogonal systems are denoted by $\Gamma_c(r)$, $\Gamma_n(r)$, $\Gamma_{M,Q}(r)$, $\Gamma_{M,B}(r)$, respectively, and the corresponding differences between the capacity limits and the values of ENR required to achieve a packet error probability of

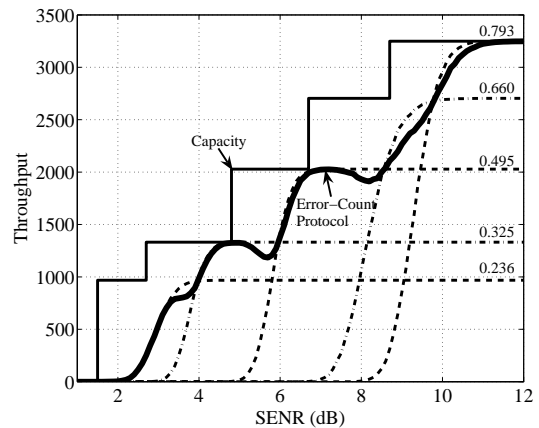


Fig. 4. Throughput for binary orthogonal modulation, noncoherent demodulation, frequency hopping, and a static Rician-fading channel with $\gamma^2 = 0.3$

10^{-2} are denoted by $\Delta_c(r)$, $\Delta_n(r)$, $\Delta_{M,Q}(r)$, and $\Delta_{M,B}(r)$, respectively. The capacity limits are compared with the values of ENR required to provide a packet error probability of 10^{-2} in Table I. For the three primary codes, the increase in ENR that is needed to decrease the packet error probability from 10^{-2} to 10^{-3} is typically not more than 0.4 dB for QAM and not more than 0.2 dB for the other forms of modulation. In wireless ad hoc networks, almost nothing is gained by reducing the packet error probability below these levels.

For an illustration of the use of capacity limits to obtain upper bounds on the throughput of a protocol, we consider frequency-hop communications with 32 binary symbols per dwell interval, binary orthogonal modulation, noncoherent demodulation, and a Rician fading channel with $\gamma^2 = 0.3$. The fading is nonselective within each frequency slot of the frequency-hop system, and the fade levels are independent in different dwell intervals. Let $\Lambda_{n,f}(r)$ denote the capacity limit in dB for this modulation and channel. The graph of $\Lambda_{n,f}(r)$ is shown in Fig. 3 along with the corresponding graphs for an AWGN channel (no fading) and a Rayleigh fading channel. From Fig. 3, we determine the capacity limit for each of the code rates available to the protocol. A hypothetical ideal protocol is provided with capacity-achieving codes of the same five rates and it is given the exact values for the channel parameters γ^2 and SENR. The ideal protocol selects the capacity-achieving code that maximizes the throughput for the given values of γ^2 and SENR. The packet success probability for a capacity-achieving code of rate r is unity if $\text{ENR} > \Lambda_{n,f}(r)$ and zero if $\text{ENR} < \Lambda_{n,f}(r)$, so the ideal protocol selects the maximum available rate r_i for which $\Lambda_{n,f}(r_i)$ is less than ENR.

The first performance results for our protocol are shown in Fig. 4 for a Rician fading channel whose parameters γ^2 and SENR are fixed but unknown to both the transmitter and receiver. These results also represent the steady-state performance of our protocol following a change in the channel parameters. Our protocol is given no information about the values of γ^2 and SENR; instead, it uses only the error count from the most recent packet transmission to select the code

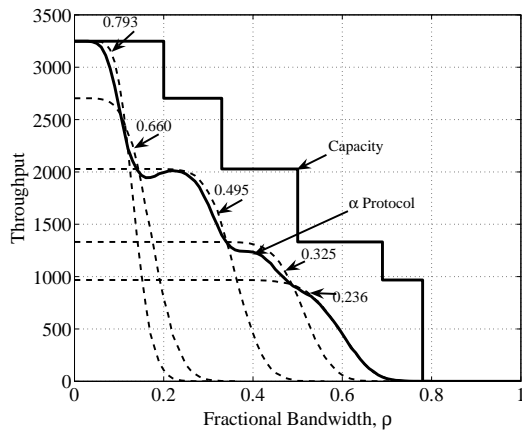


Fig. 5. Throughput for the α protocol, binary orthogonal modulation, noncoherent demodulation, frequency hopping, and a partial-band interference channel with Rician fading ($\gamma^2 = 0.3$), $\text{SENR} = 19$ dB, and $\text{SEIR} = -3$ dB.

rate for the next packet transmission. Also shown in Fig. 4 are the individual throughput curves for each of the five turbo product codes. If the same five turbo product codes are used by the ideal protocol with perfect channel state information, then the resulting throughput curve is the upper envelope of the individual throughput curves for the five codes. If the same five codes are used for both protocols, then we see from Fig. 4 that the throughput for the error-count protocol is nearly as good as the throughput for the ideal protocol, which implies that there is very little to be gained from channel measurements or additional receiver statistics. Another observation is that the differences between the throughput curve for either of the two protocols that use the turbo product codes and the throughput curve for the ideal protocol with capacity-achieving codes is less than 2 dB for most values of SENR . We also evaluated the iteration-count protocol's throughput curve for this modulation and channel, and we found that it is approximately the same as the throughput curve for the error-count protocol.

Similar conclusions are obtained from Fig. 5 for a partial-band interference channel with Rician fading. Again we see that our protocol, which is the α protocol described in [11] gives a throughput curve that is only slightly below the throughput that would be obtained from an ideal protocol with perfect channel-state information (i.e., the upper envelope of the curves shown as dashed lines). We see that capacity-achieving codes would increase the throughput substantially for an ideal protocol (especially for $0.6 \leq \rho \leq 0.8$), albeit at a cost of greater complexity than required for the turbo product codes.

V. MODELS FOR DYNAMIC CHANNELS

Each time-varying parameter for a dynamic channel is modeled by the Markov chain illustrated in Fig. 6. The state is fixed for the duration of a packet, but it can change from one packet to the next. We first consider channels for which the time-varying parameter is the propagation loss and the K states correspond to excess propagation losses L_1, L_2, \dots, L_K , in increasing order. The *excess propagation loss* is the amount in

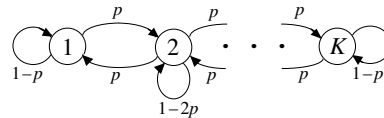


Fig. 6. Markov model for changes in channel parameters

dB by which the actual propagation loss exceeds some reference level. The reference level corresponds to state 1, so the excess path loss for state 1 is always $L_1 = 0$ dB. The results presented here are for a four-state Markov model with $p = 0.1$ and $L_k = (k-1)\Delta$ for $2 \leq k \leq 4$ and $\Delta = 1.5$ dB. We have also investigated six-state models with $\Delta = 2$ dB. The nominal value of the binary code symbol energy to noise density ratio for the AWGN channel is denoted by SENR , and the actual value when the channel is in state k is $\text{SENR}_k = \text{SENR} - L_k$. Our protocols do not know the value of SENR or the state of the channel.

For comparison with our protocols, we evaluate two hypothetical ideal protocols in which perfect information is supplied to the protocol about the past (previous state) or the future (next state). *Perfect previous-state information* consists of the exact value of the channel parameters for the previous packet transmission, and *perfect next-state information* consists of the exact value of the channel parameters for the next packet transmission (i.e., the transmission for which the code is being selected). In either case, the hypothetical protocol selects the code that maximizes the conditional expected throughput given the channel-state information.

From simulation results for the individual fixed-rate codes, such as those shown as dashed lines in Fig. 4, we can determine analytically the average throughput for each of the hypothetical ideal protocols. The throughput that is achieved by code C_i when the channel is in state k is denoted by $s(i|k)$. The transition probability $p(k|j)$ is the probability that the next state is k given that the previous state is j . First, consider the protocol with perfect previous-state information. The conditional expected throughput is

$$\bar{s}(i|j) = \sum_{k=1}^K s(i|k) p(k|j). \quad (1)$$

When the previous state is j , code C_{i_j} is selected for the next transmission if

$$\bar{s}(i_j|j) = \max\{\bar{s}(i|j) : 1 \leq i \leq n_c\}. \quad (2)$$

If π_j denotes the steady-state probability for state j in the Markov chain, then the average throughput for the protocol with perfect previous-state information is

$$\bar{S}_1 = \sum_{j=1}^K \pi_j \bar{s}(i_j|j). \quad (3)$$

Now, consider the protocol with perfect next-state information. The conditional expected throughput for code C_i given that the next state is k is $s(i|k)$. When the next state is k , code C_{i_k} is

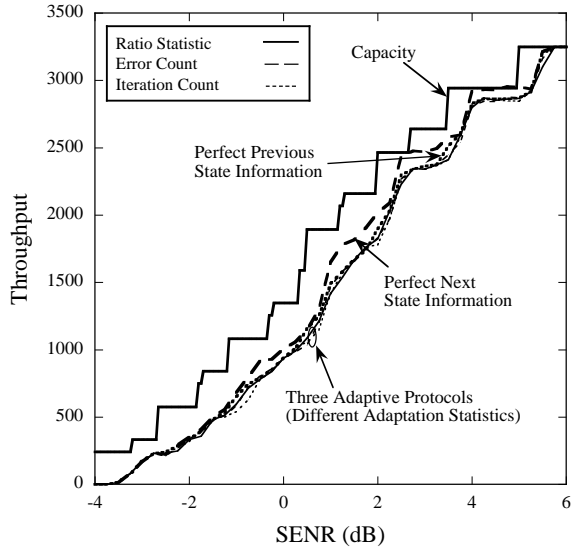


Fig. 7. Code-rate adaptation with 64-biorthogonal modulation for the four-state Markov model

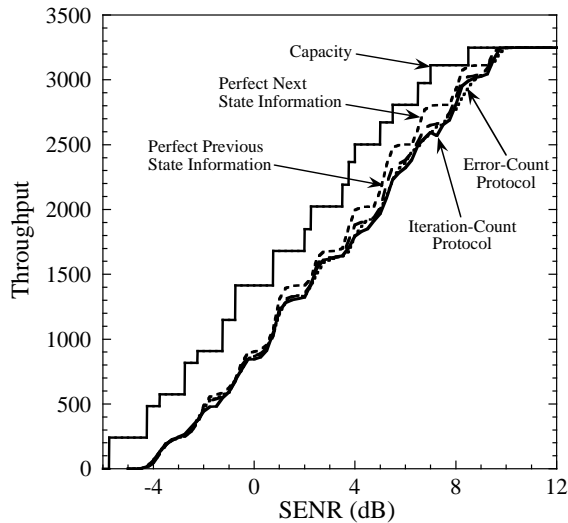


Fig. 8. Code-rate adaptation with 16-QAM for the four-state Markov model

selected for the next transmission if

$$s(i_k|k) = \max\{s(i|k) : 1 \leq i \leq n_c\}, \quad (4)$$

and the resulting average throughput for the protocol with perfect next-state information is

$$\bar{S}_2 = \sum_{k=1}^K \pi_k s(i_k|k). \quad (5)$$

For the protocol with perfect next-state information, we employ two sets of codes: the set of five turbo product codes and a set of five capacity-achieving codes of the same rates. The analytical performance results for the protocol with perfect next-state information and capacity-achieving codes represents an upper bound on the throughput for any protocol that uses any five codes with these rates. The five turbo product codes

are employed with the protocol that has perfect previous-state information to give a more realistic benchmark for our protocols. It is unrealistic to assume that the protocol will have perfect knowledge of the next channel state, so the best we can hope for in practice is to use statistics that give an accurate representation of the previous channel state. As shown in Figs. 7 and 8, each of our protocols has nearly the same throughput curve as each of the ideal protocols that are given perfect past or previous state information. Three protocols are evaluated for 64-biorthogonal modulation in Fig. 7, each of which uses a single adaptation statistic: the error count, the iteration count, or a demodulator statistic that is the ratio of the largest detector output to the second-largest output. The results for 16-QAM in Fig. 8 are for the error-count protocol and the iteration-count protocol. Our results show that more complex methods of estimating the previous channel state are not needed and will not give higher throughput than we achieve with a single adaptation statistic.

REFERENCES

- [1] Advanced Hardware Architectures, Inc., Product Specification for AHA4501 Astro 36 Mbits/sec Turbo Product Code Encoder/Decoder. Available: <http://www.aha.com>
- [2] G. Caire, G. Taricco, and E. Biglieri, "Bit-interleaved coded modulation," *IEEE Transactions on Information Theory*, vol. 44, no. 3, pp. 927–946, May 1998.
- [3] S. Dolinar and D. Divsalar, "Weight distributions for turbo codes using random and nonrandom permutations," *JPL TDA Progress Report 42-122*, pp. 56–65, August 1995.
- [4] S. Le Goff, A. Glaviuex, and C. Berrou, "Turbo-codes and high spectral efficiency modulation," *Proceedings of the 1994 IEEE International Conference on Communications*, pp. 645–649, 1994.
- [5] W. G. Phoel, J. A. Pursley, M. B. Pursley, and J. S. Skinner, "Frequency-hop spread spectrum with quadrature amplitude modulation and error-control coding," *Proceedings of the 2004 IEEE Military Communications Conference*, Nov. 2004.
- [6] M. B. Pursley and T. C. Royster, IV, "Coding alternatives for high-rate direct-sequence spread spectrum," *Proceedings of the 2004 IEEE Military Communications Conference*, Nov. 2004.
- [7] M. B. Pursley and T. C. Royster, IV, "Adaptive coding for high-rate direct-sequence spread spectrum," *Proceedings of the 2005 IEEE International Conference on Wireless Networks, Communications, and Mobile Computing (Maui, HI)*, vol. 1, pp. 624–629, June 2005.
- [8] M. B. Pursley, T. C. Royster, IV, and J. S. Skinner, "Adaptive transmission for opportunistic use of spectrum," *Proceedings of the 2005 International Symposium on Communication Theory and Applications (Ambleside, UK)*, pp. 124–129, July 2005.
- [9] M. B. Pursley, T. C. Royster, IV, and J. S. Skinner, "Protocols for the selection, adjustment, and adaptation of transmission parameters in dynamic spectrum access networks," *Proceedings of the 2005 IEEE International Symposium on New Frontiers in Dynamic Spectrum Access Networks (Baltimore)*, pp. 649–657, November 2005.
- [10] M. B. Pursley and J. S. Skinner, "Decoding strategies for turbo product codes in frequency-hop wireless communications," *Proceedings of the 2003 IEEE International Conference on Communications (Anchorage, AK)*, vol. 4, pp. 2963–2968, May 2003.
- [11] M. B. Pursley and J. S. Skinner, "Adaptive coding for mobile ad hoc networks with frequency-hop transmission and soft-decision decoding," *Proceedings of the 2005 IEEE International Conference on Wireless Networks, Communications, and Mobile Computing (Maui, HI)*, vol. 2, pp. 1418–1423, June 2005.